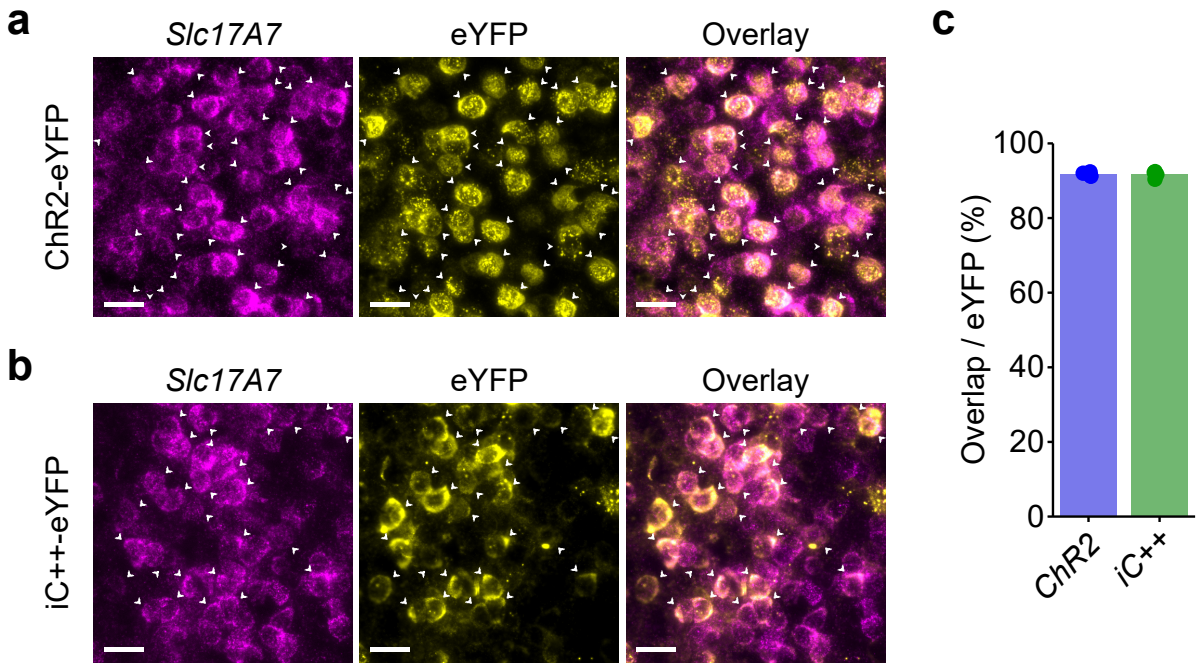

Supplementary Fig. 1. Expression of ChR2-eYFP and iC++-eYFP in mPFC glutamatergic neurons.

(a) Fluorescence *in situ* hybridization (FISH) was performed for *Slc17A7* (gene encoding the vesicular glutamate transporter 1, left) and *eYFP* (middle) in the mPFC of C57BL/6J mice injected with AAV-CaMKII-ChR2-eYFP. Right, overlay of both channels. Arrowheads indicate co-labeled cells. Scale bars, 25 μm.

(b) FISH was performed for *Slc17A7* (gene encoding the vesicular glutamate transporter 1, left panel) and *eYFP* (middle) in the mPFC of C57BL/6J mice injected with AAV-CaMKII-Cre and AAV-DIO-iC++-eYFP. Right, overlay of both channels. Arrowheads indicated co-labeled cells. Scale bars, 25 μm.

(c) Percentage of *eYFP*+ neurons expressing *Slc17A7* in mice injected with ChR2-eYFP or iC++-eYFP. ChR2, 7432 cells from n = 4 mice; iC++, 4575 cells from n = 4 mice.

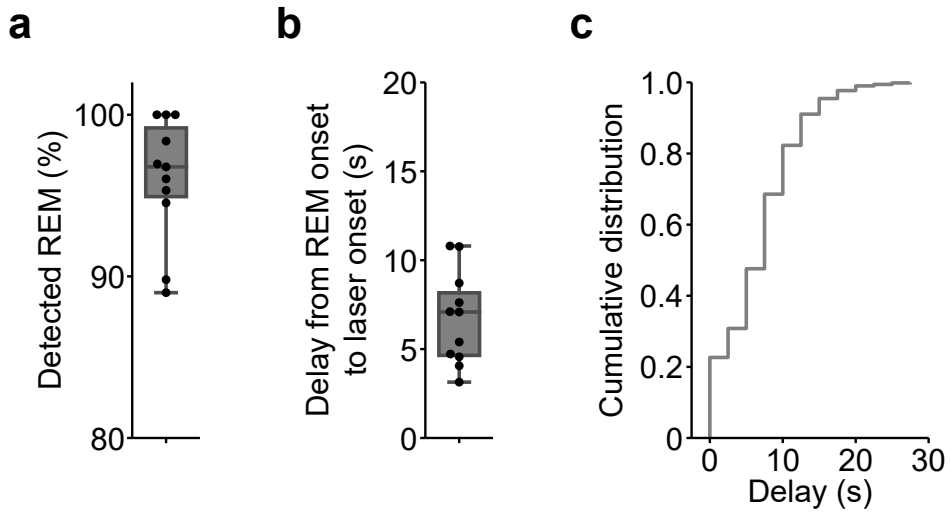

Supplementary Fig. 2. Validation of closed-loop REM sleep detection.
(a) Percentage of REM sleep episodes detected by the closed-loop stimulation system. We validated the closed-loop system using the data set for mPFC Pyr neuron activation (**Fig. 2**, n = 11 mice). Box plot (see **Methods** for definition); dots, individual mice.
(b) Delay between the onset of (offline annotated) REM sleep and online detection. n = 11 mice. Box plot; dots, individual mice.
(c) Cumulative distribution of delay times between REM onset and laser onset across all detected REM sleep episodes in the dataset; n = 1435 episodes.

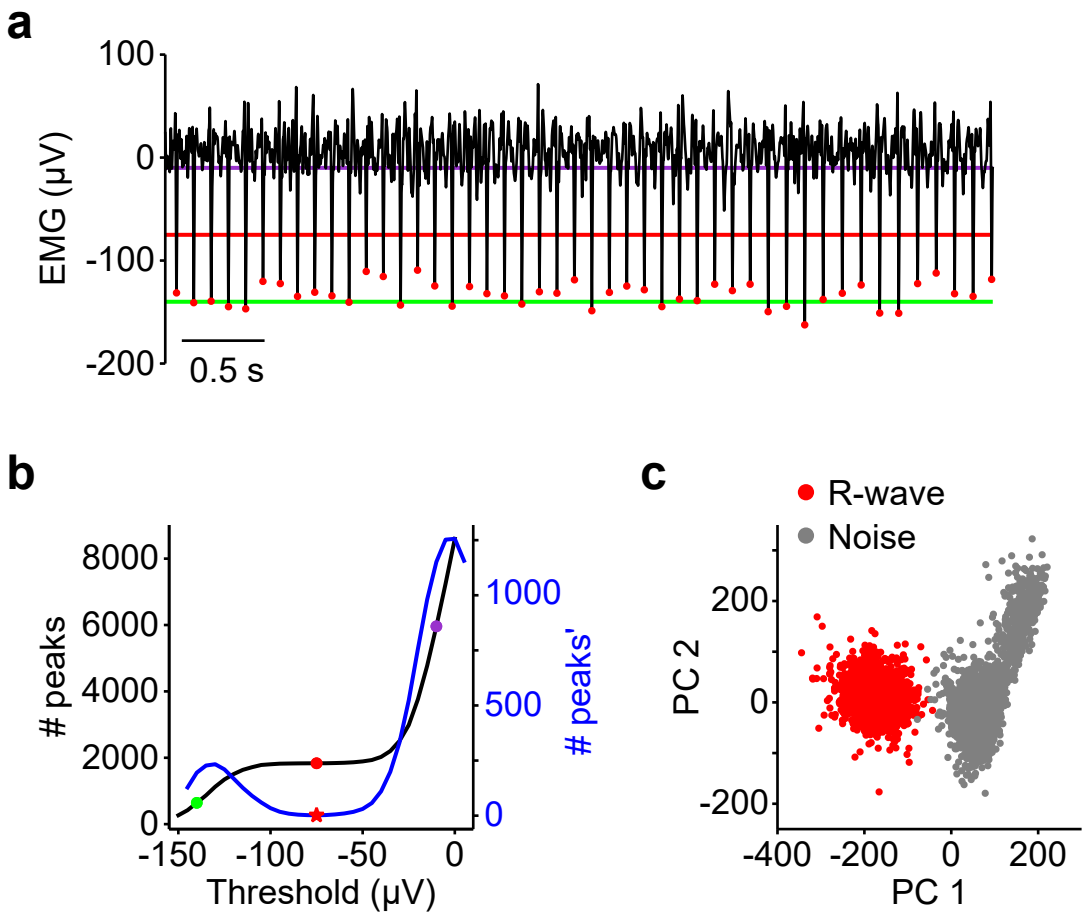

Supplementary Fig. 3. Heart rate detection using EMG.
(a) EMG during an example REM sleep episode. Red dots indicate automatically detected R-waves of the heartbeat, i.e., negative peaks below the red line (threshold). Green line, low threshold detecting only few peaks; purple line, high threshold overlapping with noise peaks.
(b) Number of detected peaks as a function of the threshold. The black line shows the number of peaks (y-axis) for the whole REM sleep episode in **(a)** for different threshold values (x-axis). The colored dots indicate the number of peaks for the three different thresholds (green, red, and purple lines in **(a)**). The blue curve represents the derivative of the black curve (#peaks'). The optimal threshold corresponds to the minimum of the blue line (red star).
(c) PCA (principal component analysis) of all waveforms below the purple threshold. Within the PC space, R-waves, defined as peaks below the red line, are well separated from the remaining noise waveforms (gray).

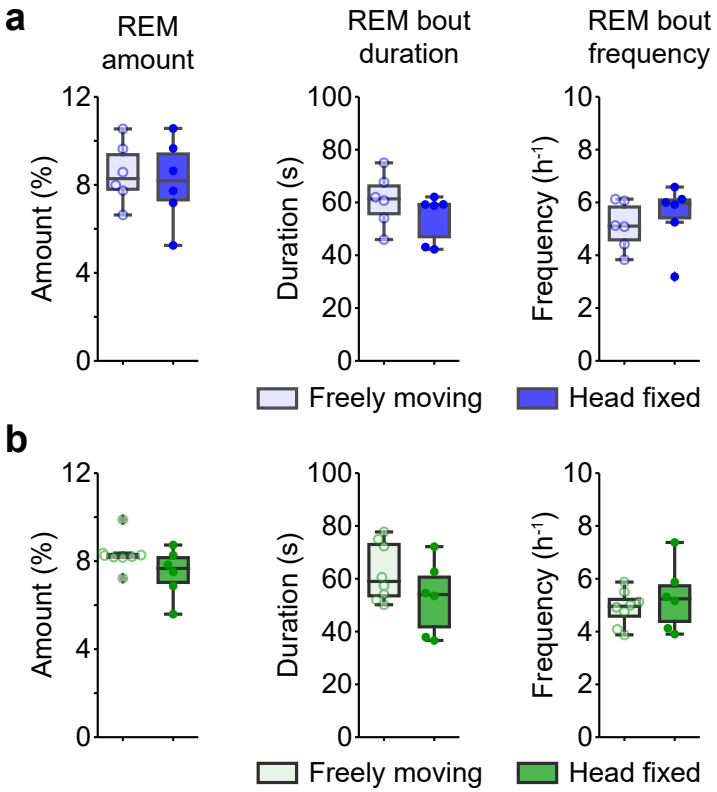

Supplementary Fig. 4. REM sleep in the head-fixed mice.
(a) Percentage (left), duration (middle), and frequency of REM sleep (right) in baseline recordings without laser stimulation in freely-moving and head-fixed mice expressing ChR2 in mPFC Pyr neurons; percentage, T(10) = -0.3643, P = 0.7232, Cohen's d = 0.2103; duration, T(10) = -1.2282, P = 0.2475, Cohen's d = 0.7091; frequency, T(10) = 0.6521, P = 0.5291, Cohen's d = 0.3765; freely-moving, n = 6; head-fixed, n = 6 mice. Box plots; dots, individual mice.
(b) Percentage (left), duration (middle), and frequency of REM sleep (right) in baseline recordings without laser stimulation in freely-moving and head-fixed mice expressing iC++ in mPFC Pyr neurons; percentage, T(8.1126) = -1.6298, P = 0.1413, Cohen's d = 0.9371; duration, T(9.3587) = -1.3846, P = 0.1983, Cohen's d = 0.7745; frequency, T(7.0840) = 0.7092, P = 0.5008, Cohen's d = 0.4184; freely-moving, n = 8; head-fixed, n = 6 mice. Box plots; dots, individual mice.

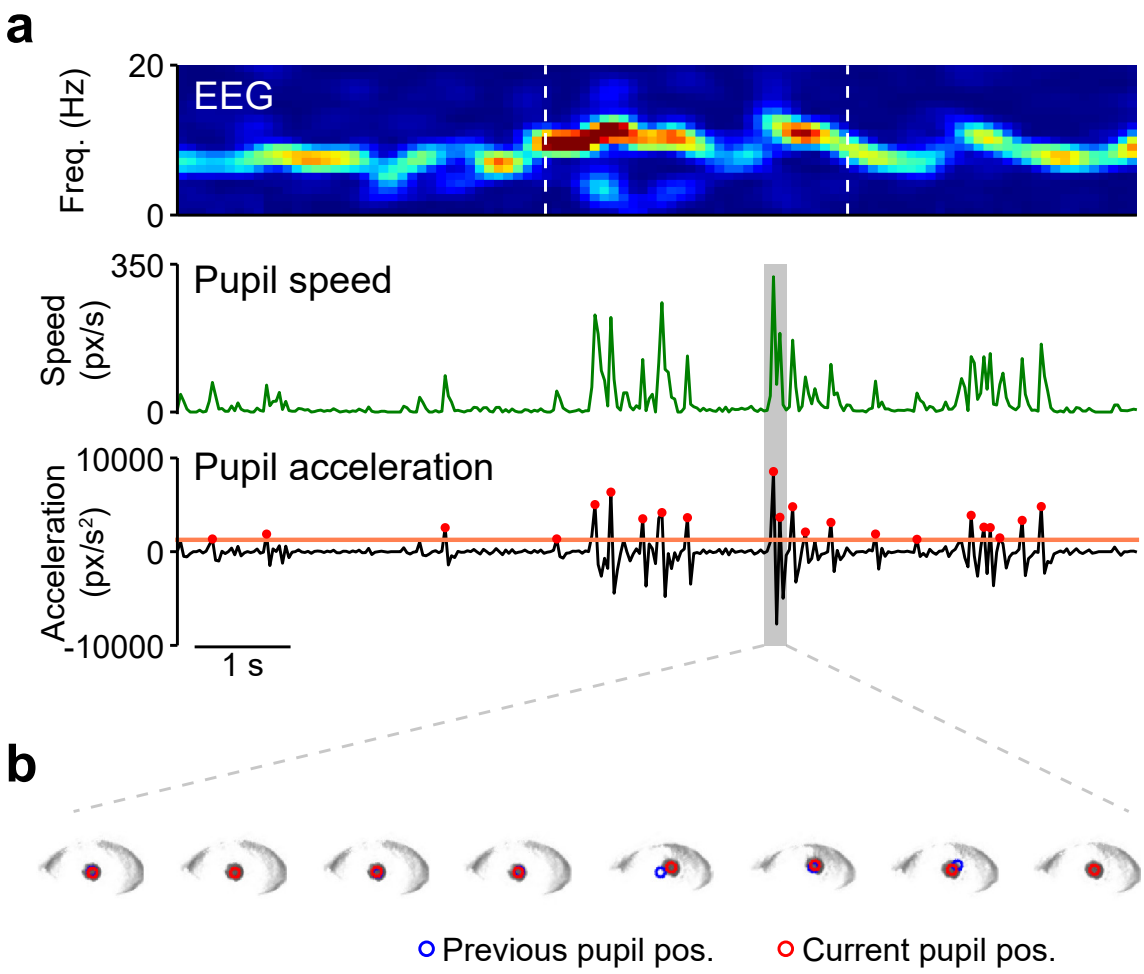

Supplementary Fig. 5. Rapid eye movement detection using video-oculography.
(a) Rapid eye movements (EMs) during REM sleep are defined as sudden accelerations in the pupil movement. For each movie frame (recorded at 30 Hz), we determined the x and y coordinates of the pupil (see **Methods**). To calculate the speed of the pupil, we first determined for each time point the pupil's change in the x and y-direction, dx and dy, between two successive video frames. The pupil speed (green line) is defined as the length of the velocity vector (dx, dy). The pupil acceleration (black line) is calculated by differentiating the speed, and rapid EMs (red dots) were identified as positive peaks of the acceleration larger than two standard deviations of the acceleration (calculated across all REM sleep episodes within the recording session; coral line). The dashed white lines on the EEG spectrogram indicate a phasic θ event. px, pixel.
(b) Consecutive movie frames (at 30 Hz) showing the eye. The red circles indicate the current pupil position; the blue circles depict the pupil position in the preceding movie frame.

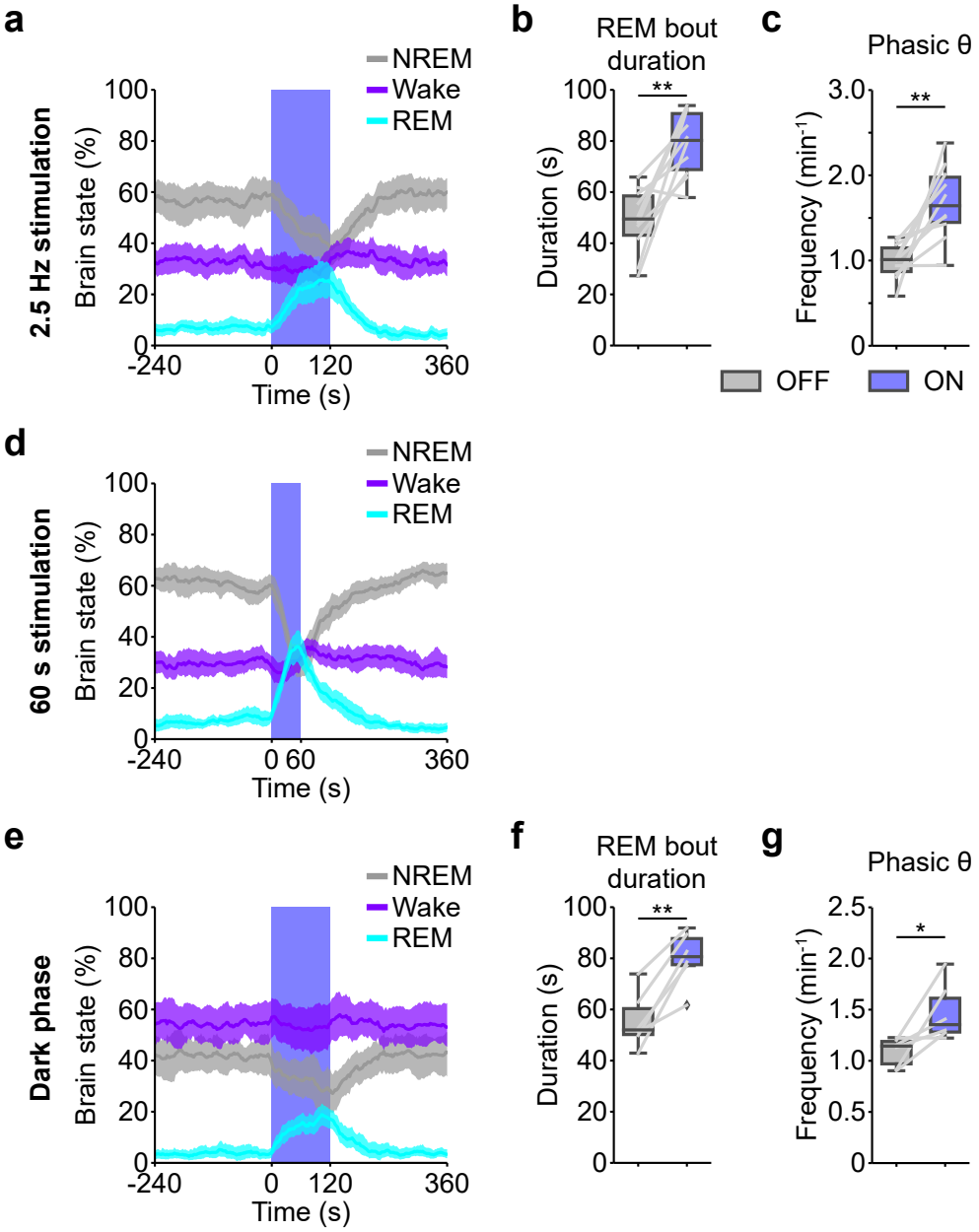

Supplementary Fig. 6. The effects of activating LH-projecting mPFC neurons on REM sleep and phasic θ events under various conditions.

(a) Percentage of all brain states before, during, and after open-loop stimulation with 2.5 Hz. Blue patch, 120 s laser stimulation interval. 2-way repeated-measures (rm) ANOVA comparing the mean percentage of each brain state during the laser interval with that during the preceding 120 s baseline interval; interaction (state x laser), F(2, 18) = 21.9467, P = 0.0002, η^2_G = 0.4096; t-tests with Holm-Bonferroni correction; baseline vs laser: REM, T(9) = 5.4817, P = 0.0012, Hedges' g = 2.1696; wake, T(9) = -2.3121, P = 0.0461, Hedges' g = -0.4410; NREM, T(9) = -4.2789, P = 0.0041, Hedges' g = -1.5184. n = 10 mice. Lines, averages across mice; shadings, 95% CIs.

(b) Duration of REM sleep episodes with (ON) and without (OFF) closed-loop laser stimulation with 2.5 Hz. Paired t-test; T(9) = 4.7928, P = 0.0010, Cohen's d = 2.3703; n = 10 mice. Box plots; lines, individual mice.

(c) Frequency of phasic θ events during REM sleep episodes with and without closed-loop laser stimulation with 2.5 Hz. Paired t-test; T(9) = 4.1043, P = 0.0027, Cohen's d = 2.0343; n = 10 mice. Box plots; lines,

individual mice.
(d) Percentage of all brain states before, during, and after open-loop stimulation with 5 Hz, lasting for 60 s. Blue patch, 60 s laser stimulation interval. 2-way rm ANOVA; interaction (state x laser), F(2, 10) = 56.7149, P = 0.0004, η^2_G = 0.8124; t-tests with Holm-Bonferroni correction; baseline vs laser: REM, T(5) = 7.3078, P = 0.0015, Hedges' g = 3.8620; wake, T(5) = -2.0508, P = 0.0955, Hedges' g = -0.9137; NREM, T(5) = -13.3703, P = 0.0001, Hedges' g = -4.4879. n = 6 mice. Lines, averages across mice; shadings, 95% CIs.
(e) Percentage of all brain states before, during, and after open-loop stimulation in the dark phase (5 Hz). Blue patch, 120 s laser stimulation interval. 2-way rm ANOVA; interaction (state x laser), F(2, 10) = 27.7342, P = 0.0001, η^2_G = 0.2925; t-tests with Holm-Bonferroni correction; baseline vs laser: REM, T(5) = 7.9886, P = 0.0015, Hedges' g = 3.6769; wake, T(5) = -0.6365, P = 0.5525, Hedges' g = -0.0793; NREM, T(5) = -4.7735, P = 0.0100, Hedges' g = -1.1810. n = 6 mice. Lines, averages across mice; shadings, 95% CIs.
(f) Duration of REM sleep episodes with (ON) and without (OFF) closed-loop laser stimulation in the dark phase. Paired t-test; T(5) = 6.4408, P = 0.0013, Cohen's d = 2.2589; n = 6 mice. Box plots; lines, individual mice.
(g) Frequency of phasic θ events during REM sleep episodes with and without closed-loop stimulation in the dark phase. Paired t-test; T(5) = 2.9916, P = 0.0304, Cohen's d = 1.7026; n = 6 mice. Box plots; lines, individual mice. *P<0.05, **P<0.01.

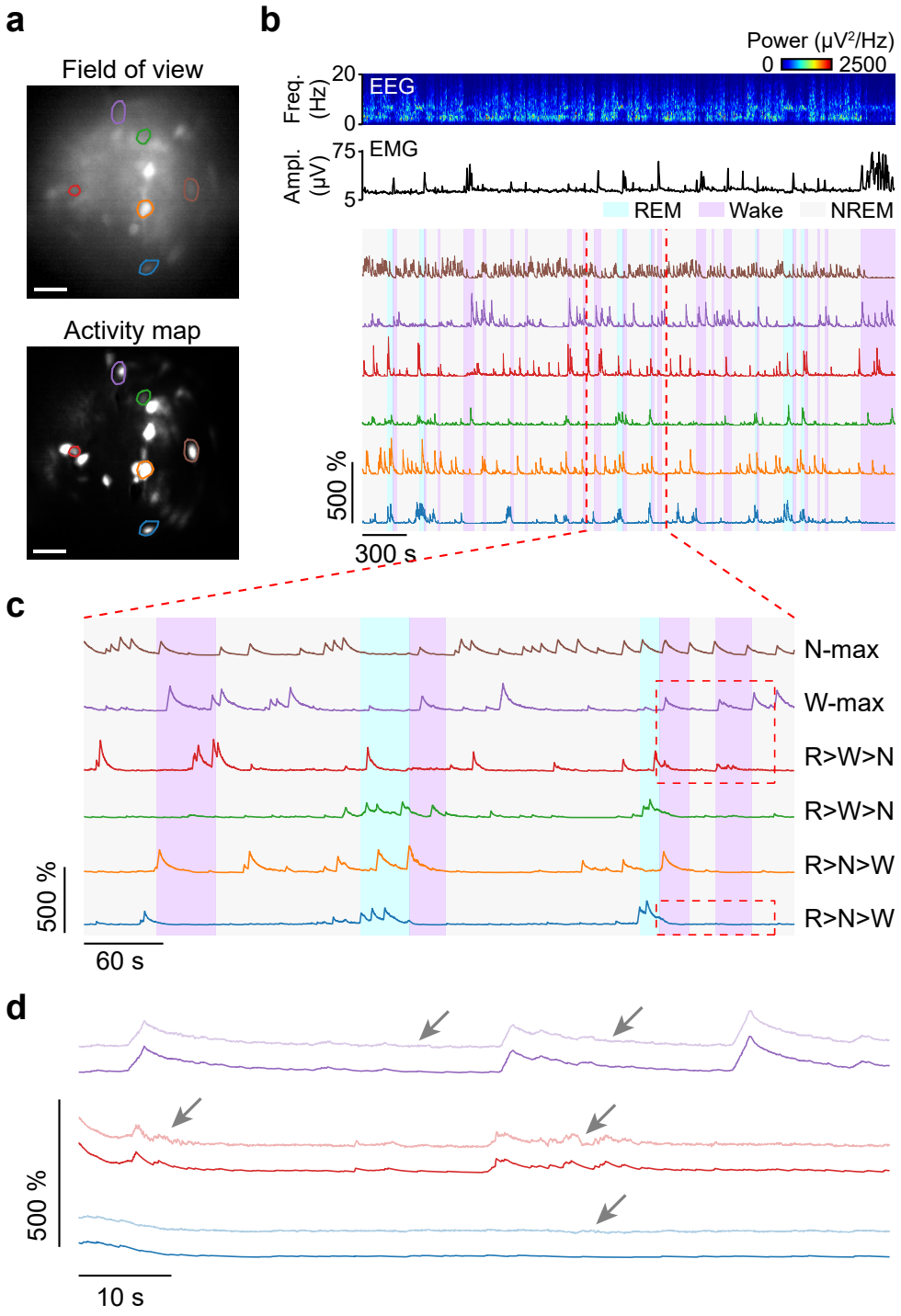

Supplementary Fig. 7. Activity of LH-projecting mPFC neurons during sleep.
(a) Field of the view and pixel-wise activity map of an example recording session. Colored polygons, example regions-of-interest (ROIs). Scale bar, 50 μm.
(b) EEG power spectrogram, EMG amplitude, and ΔF/F traces for the cells (ROIs) outlined in **(a)** during sleep.
(c) Enlarged view of ΔF/F traces. The subclass of each cell is indicated on the right.
(d) ΔF/F traces were denoised using the OASIS algorithm with an AR(1) model (**Methods**). The denoised ΔF/F traces within the red boxes in **(c)** are compared with the raw ΔF/F signals (pale colors) on an expanded time scale. For better visibility, the raw ΔF/F traces are shifted upwards. Arrows indicate areas in the fluorescence traces with noticeable denoising effect.

Supplementary Table 1. Summary of statistical results for Figures and Extended Data Figures

Each column in the table (Supplementary Table 1.xlsx) lists the

- figure/Extended Data figure reference ('Figure'),
- statistical test for group analysis ('Group analysis'),
- statistic and degrees of freedom (DOFs) for group analysis ('Statistic'),
- P-value for group analysis ('P-value'),
- effect size for group analysis ('Effect size'),
- comparisons ('Comparisons'),
- statistical test for pairwise tests ('Pairwise tests'),
- statistic and DOFs for pairwise tests ('Statistic'),
- P-values for pairwise tests ('P-value'),
- effect size for pairwise tests ('Effect size'),
- test type ('Tail'),
- sample size ('Sample size'),
- subjects ('Subjects').

Supplementary Table 2. Statistical information on imaged mPFC→LH cells.
The table (Supplementary Table 2.xlsx) provides for each imaged cell (ID)

- the mouse ID ('Mouse'),
- number of sessions ('#Sessions'),
- recording duration ('Recording duration (min)'),
- total duration of REM sleep ('Total REM (min)'),
- total duration of Wake ('Total Wake (min)'),
- total duration of NREM sleep ('Total NREM (min)'),
- number of REM sleep episodes ('#REM'),
- number of Wake episodes ('#Wake'),
- number of NREM sleep episodes ('#NREM'),
- average duration of REM sleep episodes ('REM duration (s)'),
- average duration of NREM sleep episodes ('NREM duration (s)'),
- average duration of Wake episodes ('Wake duration (s)'),
- subclass type ('Type'),
- Average $\Delta F/F$ activity (z-scored) for REM, Wake, NREM ('DF/F (z-scored) for REM, Wake, NREM'),
- F-value for one-way ANOVA ('F ANOVA'),
- P-value for ANOVA ('P ANOVA'),
- Tukey's HSD post-hoc test ('Tukey (N∼R, N∼W, R∼W)').

Supplementary Table 3. Statistical results for analysis of $\Delta F/F$ activity during brain state transitions.

For each subclass of mPFC→LH cells in **Fig. 5e**, we determined whether their activity (discretized in 10 s bins) was significantly modulated during brain state transitions (ranging from -60 s before to 30 s after the transition) using one-way rm ANOVA (**Methods**). Using pairwise t-tests with Holm-Bonferroni correction, we determined for which 10 s bins the activity significantly differed from the initial baseline bin (-60 to -50 s). The time point for each bin was set to its midpoint. For each transition, we provide the ANOVA results and the results for the pairwise t-tests comparing the baseline bin (Bsl) with each consecutive bin (X).

(a-d) Results for NREM→REM (NR), REM→Wake (RW), NREM→Wake (NW), and Wake→NREM (WN) transitions (R>W>N, n = 36; R>N>W, n = 43; Wake-max, n = 34; NREM-max, n = 16 cells; n = 8 mice).

(a) NREM → REM

Type	F	P	η^2_G	Transition
R>W>N	26.9255	0.0000	0.3950	NR
R>N>W	15.6909	0.0000	0.2024	NR
W-max	3.4661	0.0219	0.0654	NR
N-max	2.5652	0.0478	0.1078	NR

Type	Bsl	X	T	P	Hedges' g	Transition
R>W>N	-55.0	-45.0	-0.0469	1.0000	-0.0091	NR
R>W>N	-55.0	-35.0	-0.4787	1.0000	-0.0931	NR
R>W>N	-55.0	-25.0	0.0842	1.0000	0.0184	NR
R>W>N	-55.0	-15.0	-1.6937	1.0000	-0.3883	NR
R>W>N	-55.0	-5.0	-3.7120	0.0121	-0.8953	NR
R>W>N	-55.0	5.0	-6.1294	0.0000	-1.4760	NR
R>W>N	-55.0	15.0	-7.0987	0.0000	-1.6764	NR
R>W>N	-55.0	25.0	-7.1893	0.0000	-1.5408	NR
R>N>W	-55.0	-45.0	1.0996	1.0000	0.1681	NR
R>N>W	-55.0	-35.0	0.0894	1.0000	0.0121	NR
R>N>W	-55.0	-25.0	-0.1363	1.0000	-0.0277	NR
R>N>W	-55.0	-15.0	-3.2658	0.0348	-0.6314	NR
R>N>W	-55.0	-5.0	-3.8390	0.0078	-0.7844	NR
R>N>W	-55.0	5.0	-4.6797	0.0008	-1.0630	NR
R>N>W	-55.0	15.0	-4.6865	0.0008	-1.0164	NR
R>N>W	-55.0	25.0	-4.6633	0.0008	-0.9977	NR
W-max	-55.0	-45.0	0.8419	1.0000	0.1280	NR
W-max	-55.0	-35.0	1.7015	1.0000	0.3871	NR
W-max	-55.0	-25.0	0.6511	1.0000	0.1461	NR
W-max	-55.0	-15.0	-0.3726	1.0000	-0.0772	NR
W-max	-55.0	-5.0	-1.2976	1.0000	-0.3004	NR
W-max	-55.0	5.0	-1.6679	1.0000	-0.4171	NR
W-max	-55.0	15.0	-1.6813	1.0000	-0.4501	NR
W-max	-55.0	25.0	-1.9257	1.0000	-0.5146	NR
N-max	-55.0	-45.0	0.1734	1.0000	0.0424	NR
N-max	-55.0	-35.0	-0.5981	1.0000	-0.1859	NR
N-max	-55.0	-25.0	-0.3433	1.0000	-0.1320	NR
N-max	-55.0	-15.0	0.1513	1.0000	0.0559	NR
N-max	-55.0	-5.0	0.4106	1.0000	0.1071	NR
N-max	-55.0	5.0	1.2581	1.0000	0.4407	NR
N-max	-55.0	15.0	2.0878	1.0000	0.7553	NR
N-max	-55.0	25.0	2.2257	1.0000	0.8919	NR

(b) REM → Wake

Type	F	P	η^2_G	Transition
R>W>N	2.9086	0.0172	0.0632	RW
R>N>W	16.2332	0.0000	0.1939	RW
W-max	23.8191	0.0000	0.3229	RW
N-max	1.0169	0.3824	0.0447	RW

Type	Bsl	X	T	P	Hedges' g	Transition
R>W>N	-55.0	-45.0	0.8051	1.0000	0.1434	RW
R>W>N	-55.0	-35.0	-0.1518	1.0000	-0.0319	RW
R>W>N	-55.0	-25.0	-1.2646	1.0000	-0.2772	RW
R>W>N	-55.0	-15.0	-1.9345	1.0000	-0.3626	RW
R>W>N	-55.0	-5.0	-1.5945	1.0000	-0.3491	RW
R>W>N	-55.0	5.0	-1.4536	1.0000	-0.3837	RW
R>W>N	-55.0	15.0	0.3970	1.0000	0.1104	RW
R>W>N	-55.0	25.0	1.2524	1.0000	0.3263	RW
R>N>W	-55.0	-45.0	-0.4704	1.0000	-0.0820	RW
R>N>W	-55.0	-35.0	-0.8392	1.0000	-0.1658	RW
R>N>W	-55.0	-25.0	-1.5587	1.0000	-0.2984	RW
R>N>W	-55.0	-15.0	-2.5040	0.2925	-0.4885	RW
R>N>W	-55.0	-5.0	-2.9548	0.1022	-0.5516	RW
R>N>W	-55.0	5.0	0.4092	1.0000	0.0726	RW
R>N>W	-55.0	15.0	7.2965	0.0000	1.3358	RW
R>N>W	-55.0	25.0	5.1310	0.0002	0.9613	RW
W-max	-55.0	-45.0	-0.5943	1.0000	-0.0789	RW
W-max	-55.0	-35.0	-1.7539	1.0000	-0.2312	RW
W-max	-55.0	-25.0	-1.0730	1.0000	-0.1617	RW
W-max	-55.0	-15.0	-1.1400	1.0000	-0.1532	RW
W-max	-55.0	-5.0	-1.4347	1.0000	-0.2291	RW
W-max	-55.0	5.0	-7.5432	0.0000	-1.5109	RW
W-max	-55.0	15.0	-5.9178	0.0000	-1.4740	RW
W-max	-55.0	25.0	-4.8354	0.0007	-1.2860	RW

(c) NREM → Wake

Type	F	P	η^2_G	Transition
R>W>N	17.2274	0.0000	0.2869	NW
R>N>W	35.9934	0.0000	0.3912	NW
W-max	33.6118	0.0000	0.4579	NW
N-max	2.5351	0.0675	0.1276	NW

Type	Bsl	X	T	P	Hedges' g	Transition
R>W>N	-55.0	-45.0	-2.3957	0.3311	-0.3629	NW
R>W>N	-55.0	-35.0	-0.8622	1.0000	-0.1560	NW
R>W>N	-55.0	-25.0	-1.5288	1.0000	-0.3518	NW
R>W>N	-55.0	-15.0	-2.1308	0.4825	-0.4980	NW
R>W>N	-55.0	-5.0	-3.8371	0.0120	-0.8572	NW
R>W>N	-55.0	5.0	-6.8338	0.0000	-1.6209	NW
R>W>N	-55.0	15.0	-4.9180	0.0006	-1.2532	NW
R>W>N	-55.0	25.0	-4.2875	0.0038	-1.0842	NW
R>N>W	-55.0	-45.0	-0.1673	1.0000	-0.0275	NW
R>N>W	-55.0	-35.0	-0.8800	1.0000	-0.1715	NW
R>N>W	-55.0	-25.0	-3.2319	0.0269	-0.6702	NW
R>N>W	-55.0	-15.0	-4.6539	0.0007	-0.9503	NW
R>N>W	-55.0	-5.0	-3.7380	0.0089	-0.8433	NW
R>N>W	-55.0	5.0	0.7405	1.0000	0.1657	NW
R>N>W	-55.0	15.0	9.0927	0.0000	2.0389	NW
R>N>W	-55.0	25.0	6.4188	0.0000	1.2727	NW
W-max	-55.0	-45.0	0.8377	1.0000	0.1132	NW
W-max	-55.0	-35.0	0.5977	1.0000	0.1203	NW
W-max	-55.0	-25.0	1.4834	1.0000	0.3220	NW
W-max	-55.0	-15.0	0.9916	1.0000	0.2413	NW
W-max	-55.0	-5.0	0.2965	1.0000	0.0630	NW
W-max	-55.0	5.0	-7.1854	0.0000	-1.7825	NW
W-max	-55.0	15.0	-6.1578	0.0000	-1.5523	NW
W-max	-55.0	25.0	-5.0415	0.0003	-1.2730	NW

(d) Wake → NREM

Type	F	P	η^2_G	Transition
R>W>N	4.2618	0.0013	0.0571	WN
R>N>W	4.5395	0.0008	0.0466	WN
W-max	5.7117	0.0021	0.0617	WN
N-max	7.0776	0.0003	0.2127	WN

Type	Bsl	X	T	P	Hedges' g	Transition
R>W>N	-55.0	-45.0	-0.0559	1.0000	-0.0066	WN
R>W>N	-55.0	-35.0	0.5510	1.0000	0.0806	WN
R>W>N	-55.0	-25.0	1.7942	1.0000	0.2970	WN
R>W>N	-55.0	-15.0	2.6180	0.3764	0.4953	WN
R>W>N	-55.0	-5.0	3.1306	0.1089	0.4938	WN
R>W>N	-55.0	5.0	2.4702	0.4815	0.4731	WN
R>W>N	-55.0	15.0	3.4334	0.0496	0.7553	WN
R>W>N	-55.0	25.0	3.6415	0.0304	0.6914	WN
R>N>W	-55.0	-45.0	1.9359	1.0000	0.2106	WN
R>N>W	-55.0	-35.0	2.5381	0.4185	0.4179	WN
R>N>W	-55.0	-25.0	3.2359	0.0758	0.5382	WN
R>N>W	-55.0	-15.0	0.8532	1.0000	0.1527	WN
R>N>W	-55.0	-5.0	0.6830	1.0000	0.1034	WN
R>N>W	-55.0	5.0	0.8729	1.0000	0.1156	WN
R>N>W	-55.0	15.0	-0.4567	1.0000	-0.0859	WN
R>N>W	-55.0	25.0	-0.8108	1.0000	-0.1355	WN
W-max	-55.0	-45.0	2.2019	0.6465	0.2222	WN
W-max	-55.0	-35.0	1.9045	0.9839	0.2517	WN
W-max	-55.0	-25.0	2.3319	0.5711	0.3303	WN
W-max	-55.0	-15.0	2.4484	0.4760	0.4052	WN
W-max	-55.0	-5.0	2.1911	0.6465	0.3743	WN
W-max	-55.0	5.0	3.0546	0.1464	0.6051	WN
W-max	-55.0	15.0	2.8660	0.2155	0.5877	WN
W-max	-55.0	25.0	3.2152	0.1020	0.7289	WN
N-max	-55.0	-45.0	-1.0645	1.0000	-0.2576	WN
N-max	-55.0	-35.0	0.6556	1.0000	0.1576	WN
N-max	-55.0	-25.0	0.8689	1.0000	0.2063	WN
N-max	-55.0	-15.0	0.6994	1.0000	0.1434	WN
N-max	-55.0	-5.0	0.2325	1.0000	0.0507	WN
N-max	-55.0	5.0	-0.8755	1.0000	-0.1940	WN
N-max	-55.0	15.0	-2.7310	0.4330	-0.9110	WN
N-max	-55.0	25.0	-3.9417	0.0444	-1.2808	WN

Supplementary Table 4. Index of brain region abbreviations
The table provides definitions of all abbreviations used in Fig. 6.

Abbreviation	Brain region
Cg1	Cingulate cortex, area 1
Cg2	Cingulate cortex, area 2
M2	Secondary motor cortex
FRA	Frontal association cortex
PL	Prelimbic cortex
IL	Infralimbic cortex
MO	Medial orbital cortex
VO	Ventral orbital cortex
LO	Lateral orbital cortex
DP	Dorsal peduncular cortex
AIV	Agranular insular cortex, ventral part
Cl	Claustrum
RSGs	Retrosplenial granular cortex
RSD	Retrosplenial dysgranular cortex
V2MM	Secondary visual cortex, mediomedial area
Pir	Piriform cortex
SHi	Septohippocampal nucleus
LS	Lateral septal nucleus
Ld	Lambdoid septal zone
MS	Medial septal nucleus
VDB	Nucleus of the vertical limb of the diagonal band
HDB	Nucleus of the horizontal limb of the diagonal band
VP	Ventral pallidum
MCPO	Magnocellular preoptic nucleus
MPA	Medial preoptic area
LPO	Lateral preoptic area
AOM	Anterior olfactory area, medial part
DTT	Dorsal tenia tecta
VTT	Ventral tenia tecta
AchSh	Accumbens nucleus, shell
AV	Anteroventral thalamic nucleus
AM	Anteromedial thalamic nucleus
AD	Anterodorsal thalamic nucleus
PVA	Paraventricular thalamic nucleus, anterior part
CM	Central medial thalamic nucleus
MD	Mediodorsal thalamic nucleus
RE	Reuniens thalamic nucleus
Sub	Submedius thalamic nucleus
LH	Lateral hypothalamic area
PH	Posterior hypothalamic nucleus
CA1	Field CA1 of the hippocampus
CA2	Field CA2 of the hippocampus
DS	Dorsal subiculum
Ent	Endopiriform claustrum
BLA	Basolateral amygdaloid nucleus, anterior part
BLP	basolateral amygdaloid nucleus, posterior part
EA	Extended amygdala
PAG	Periaqueductal gray

Supplementary Video 1. Induction of REM sleep by optogenetic activation of mPFC Pyr neurons.
The video shows a top-view of the animal's home cage together with the timing of the laser (120 s, 5 Hz), EEG spectrogram, EMG amplitude and color-coded brain states. In trials 1 and 2, laser stimulation was initiated during NREM sleep. In the last trial, laser stimulation overlaps with wakefulness. The video is shown at 15x speedup.

Supplementary Video 2. Rapid eye movements during REM sleep.
Video recording of the eye in a head-fixed mouse (left). The detected pupil position is indicated by a red dot. The panel on the right shows the EEG spectrogram, EMG amplitude, and pupil speed (green). The time points of rapid eye movements (defined as sudden accelerations in the pupil speed; **Methods**) are indicated as blue ticks.

Supplementary Video 3. *In vivo* calcium imaging of mPFC→LH neurons.
Calcium activity of mPFC→LH neurons recorded using Miniscope (left) along with EEG spectrogram, EMG amplitude, and $\Delta F/F$ calcium traces. Several cells (colored ROIs) are drown on top of the calcium video. The calcium traces (right) are represented using the same color code. The video is shown at 30x speedup.